Comparison of Bone Robustness Between Fore- and Hindlimb in Neonatal and Infant Galago

Jeremy Busken

Department of Biology, University of Akron

Honors Thesis

Dr. Jesse Wyatt Young

4/21/2023

Keywords:

Primates, Galagos, *G. senegalensis, G. moholi,* Cortical Bone, ImageJ, Biomaterial, Morphology, Material Properties, quadrupedal, leapers

Abstract:

According to Wolff's law, bone is constantly subject to change based on loading pattern (Ruff et al., 2006). Those subjected to greater stress become more robust by increasing bone mineral density and often changing geometric properties. Previous studies of primate anatomy have found significant differences in bone robustness between the fore- and hindlimbs in adult leaping primates. Because leaping primates, such as *Galago senegalensis* and *Galago moholi*, subject their hindlimbs to much greater stress, this difference in robustness may come as a result of bone functional adaptation/Wolff's law. This study sought to investigate this possibility by testing neonatal and infant primates which would not mature enough to subject their bones to any significant loading stress. Seven infant and five neonatal *G. senegalensis* and *G. moholi* had their bones extracted, and then subjected to micro CT scans and three-point bending testing. Our data shows that the hindlimbs of Galagos display more robust geometric properties when compared to their forelimbs, however, it did not find any difference in either the material properties or whole bone properties. These findings demonstrate that some of the observed differences in robustness are present from birth and may be attributed to genetic or epigenetic factors.

Introduction:

A common misconception about bone is that bones exist as inert structures without significant changes throughout the lifespan of an organism. However, this belief is not supported by the evidence; bone exists as a dynamic structure that responds to the environment that an

organism is subjected to (Florencio-Silva et al., 2015). Wolff's law, first postulated by Julius Wolff, states that both the cortical and trabecular bone will remodel according to the loading stress (Ruff et al., 2006). While many of Wolff's original ideas are seen as outdated, the general premise that properties of bone change according to stress has held up to scrutiny. Since its original publication in 1892, studies have been conducted that identified the mechanism of this remodeling. Within the trabecular bone, the trabeculae will adapt architecture in order to maintain a greater load. Changes to the cortical bone also result from loading stress. When stresses are low, osteoclasts cause the reabsorption of minerals, and the bone becomes weaker (Florencio-Silva et al., 2015). Conversely, when stresses are high, osteoblasts deposit minerals and collagen to increase bone mineral density (BMD). These adaptations exist as an evolutionary response; those bones under constant stress will have a greater BMD and will be less likely to break, increasing the possible survival of the organism.

Material properties are often used as a general metric of overall bone robustness. For example, BMD is often used in human studies in order to track the effect of exercise on bone robustness (Ruff et al, 2006). However, material properties metrics alone cannot explain 100% of the increase in robustness that occurs during loading adaptation. Geometry properties such as cross-sectional area (CSA) and the polar section modulus (Z_{pol}), can often explain differences in overall bone robustness when material properties are similar. A study performed by Robling et al.(2002) created bending stresses in the forearm of mice and found that it resulted in an increase in bone strength of 64 to 165 percent. However, these changes could not be easily explained by a simple increase in BMD, but rather by the changes in the geometric properties of the bone. This increase was ascribed primarily to an increase in the second moment of area (I), a geometric

property. A later study by Warden et al. (2005) found similar results. Both studies found that geometric change alone could result in significant increases in overall bone strength.

Studies of bone robustness are often focused on long bones such as the femur, humerus, radius, ulna, and tibia (Robling et al., 2002; Young et al, 2018). These bones are both easy to test and subject to significant stress during most forms of primate locomotion. Several studies of adult primates have found differences in cross-sectional geometry in the long bones depending on the method of locomotion. Primates whose primary method of locomotion is leaping, such as lemurs (Indriidae) and bushbabies (Galagidae), display more robust femora than humeri. These studies have primarily found higher (CSA) and greater moments of area in the femur of leaping primates. Primates whose primary method of locomotion is quadrupedal (use of all four limbs) typically display similar robustness between the femur and humerus (Terranova CJ. 1995; Connour et al., 2000; Young et al., 2018). These differing geometric properties of bone in adult primates may be attributed to Wolff's law (bone functional adaptation) or to factors present at birth such as genetics or epigenetics causes.

Therefore, in order to test the hypothesis that these differences cannot be solely attributed to bone functional adaptations, a study has been performed by Young et al. (2018) on neonatal and infant primates. This study found significant differences in both CSA and Z_{pol} between the femur and humerus in the leaping indriid primate *Propithecus coquereli.* These results are consistent with studies of adult primates, thus indicating that these traits may have a genetic basis. However, Young et al. (2018) noted that his sample size was limited and therefore additional studies should be conducted to gain a better understanding of the subject.

This study intends to expand on the previous study by Young et al. (2018) and compare the material and geometric properties between the front and hind limbs of another leaping

primate, the *Galago*. Galagos, often called "bushbabies" as a result of their almost human cry, are a diverse group of African primates. Six genera of Galagos exist: *Euoticus, Galagoides, Galago, Paragalago, Otolemur and Sciurocheirus*. The genus *Galago,* commonly called lesser galagos, consists entirely of specialized leapers. This study focuses on the two most common lesser galagos, *G. moholi* and *G. senegalensis*. They were specifically chosen due to their powerful hind limbs and jumping ability. For example*, G. senegalensis* are capable of vertically leaping 2.25 m despite only being 130 mm tall (Hall-Craggs, 1965). This ability makes *G. senegalensis* an ideal subject as significantly more stress should be subject to the hind limbs when compared to the forelimbs. We hypothesized that bone robustness is genetically controlled, therefore, infant and neonatal *G. senegalensis* and *G. moholi* will display more robust hindlimbs compared to forelimbs, displayed through significantly different bone geometric and material properties.

Methods and Materials:

The method and materials of this study closely follow the previous study by Young et al (2018), and will only be briefly summarized here.

Cadaveric Samples:

A total of 12 specimens were obtained from Dr. Timothy Smith, Slippery Rock University, Slippery Rock, PA.). This sample consisted of ten *G. senegalensis* and two G *moholi* (**Table 1**). The ages of the specimen range from neonates to infants with no juvenile specimen obtained (where a juvenile is defined as an ecologically independent individual prior to sexual maturity). The exact age of the specimens at the time of death was not recorded and the duration

of fixation is also unknown. However, it is known that all specimens died of natural causes. After death, all specimens were preserved in 10% formalin buffer. This method prevents protein breakdown, however, it may have affected the material properties of the bone via some demineralization (Turner and Burr, 1993). Since all samples are subjected to the same formalin preservation, comparisons can be made among the specimens. Additionally, Young et al. (2018) showed that in a similar sample of neonatal indriid primates duration of formalin fixation was not significantly related to variation in material properties. However, the values obtained during this experiment cannot be used as true measures of bone material properties

#	Species	Specimen ID	Age Category
1	G *moholi*	3176	Neonate
2	G *moholi*	GSM	Infant
3	*G. senegalensis*	3008	Neonate
4	*G. senegalensis*	3009	Infant
5	*G. senegalensis*	3010	Infant
6	*G. senegalensis*	3011	Neonate
7	*G. senegalensis*	3017	Infant
8	*G. senegalensis*	3018	Infant
9	*G. senegalensis*	4005	Neonate
10	*G. senegalensis*	4007	Neonate
11	*G. senegalensis*	4012	Infant
12	*G. senegalensis*	Hisinfant2	Infant

Table 1: Specimen species, ID and ages

Long Bone Extractions:

Specimens were received as entire cadavers, rather than individual bones. Each specimen first had the limbs disarticulated, then each individual limb bone was stripped of muscle and other connective tissue. All bones present within each specimen could not be extracted. Neonatal and infant bones are often not fully ossified and created some difficulty in removal without damage to the bone. Damaged bones were not assessed for geometric and material properties. The ulna was extracted and scanned but not used in statistical analysis for this study.

Measurement and Analysis of Geometric Properties:

Cross-sectional geometry of the humerus, femur, radius, tibia, and ulna were obtained from micro-computed tomography (μCT) scans. Scans were made starting at the exact center of the diaphysis, ± 5% of the bone. Between 90-350 slices were taken for each bone, encompassing 10% of the total length of the bone. The mid-shaft of the diaphysis was studied given that it is the location of the peak bending stain and has therefore been the focus of previous studies of bone robustness (i.e., Biewener and Taylor, 1986; Young et al., 2018).

The μCT images were uploaded into NIH ImageJ (Rasband, 1997) and analyzed using the plugin BoneJ (Doube et al., 2010). The "Slice Geometry" routine of the BoneJ was used to quantify the bone mineral density (BMD) and the geometric properties of cross-sectional area (CSA) and polar selection modulus (Z_{pol}). The CSA is relevant property as it is proportional to strength in axial loading, which long bones are subjected to in both quadrupedal and leap locomotion. The polar selection modulus is relevant as it is proportional to strength in bending. Multiple bones were included in each individual μCT scan. The image was first cropped to one individual bone, then a minimum area was selected, and a "clear outside" was selected. This reduced the possible interference by removing any pixels outside the selected area. After the

image was isolated, the threshold was adjusted so that only ossified bone was selected. BoneJ provided a measurement of BMD for each individual slice. CSA or cross-sectional area is also calculated from this data. CSA is the overall cross-sectional area minus the medullary cavity. Finally, Z_{pol} or polar section modulus is determined. Z_{pol} is calculated as the polar moment of area (J) divided by the maximum radius of the cross-section (Turner and Burr, 1993). The polar moment of area or J is a common metric of the average distribution of long bone away from the central axis. All metrics were first calculated for each individual slice, then later averaged across all slices analyzed within each bone.

Measurement and Analysis of Material Properties:

In order to determine the material properties of each individual bone, a three-point bend test was performed. The three-point testing was performed by the Instron ElectroPuls E3000 material testing machine (Instron, Norwood, MA). Modification of the Instron cross-head was necessary to test samples of this size. The traditional cross head was replaced by an Instron mechanical wedge-action tensile grip attached to the sharp side of a razor blade, leaving the blunt end to make contact with the bone. This design follows previous designs of material testing in mice and other small animals (Saunders and Donahue, 2004). The bones were placed in three-point bend flexure fixtures and the support span was measured and recorded. The support span was adjusted to ensure that each bone was supported at the proximal and distal metaphyses and encompassed around 75% of the bone between the support spans. Then each bone was tested with a displacement rate of 1.24–1.27 mm/min and a data collection rate of 10 Hz following Young et al. (2018).

None of the test samples were fully fractured and each test was manually stopped. The tests were stopped after significant enough deformation occurred so that material properties such as elastic modulus, yield strength, and ultimate strength could be determined. The raw displacement and applied load data from the three-point testing and the geometric data from BoneJ were imported into Mathlab (MathWorks, Natick, MA). The program was custom-written by JWY and is similar to that used during a previous study (Young et al., 2018). The software converted deformation into strain (ϵ) and load (σ) into stress using the formula of three-point bending of hollow cylinders as established by Turner and Burr (1993). The formula for stain and load are shown below:

$$\text{Strain}(\epsilon) = \frac{12cd}{(L)^2}, \quad \text{Stress}(\sigma) = \frac{FLc}{4I}$$

The letter c represents the distance from the surface of the bone to the neutral axis/center of mass expressed and d represents the displacement of the bone, both expressed in meters. The F represents the applied force or bending load in newtons and the L is the moment arm of the bending load in meters. L is also equal to the support span. Finally, I is the second moment of area respective to the neutral axis/center of mass expressed in meters^4.

The strain output is expressed with the units mm/mm and the stress output is expressed using the units megapascals (MPa). The stress vs strain data is then smoothed and used to calculate the values of four material properties: ultimate strength, elastic modulus, yield strength, and ultimate toughness. Additionally, two measurements of whole-bone performance were calculated; ultimate and yield moment. An example stress vs stain graph is shown in **Figure 1**. The yield is the point at which stresses on the bone causing it to undergo permanent damage (Burr and Turner, 1993). The elastic modulus is equal to the (stress/strain) and expressed in Pa or N/m^2. It is equal to the slope of the line during the elastic region or the region before the yield

point. The yield strength is defined as the amount of stress withstood by the bone at the yield point. The ultimate strength is defined as the maximum stress withstood by the bone during the bend test and ultimate toughness is the area under the stress-strain curve, including both the plastic and elastic region. The Ultimate moment was calculated as support span length (L) multiplied by the applied load (N) at the point of ultimate stress. The yield moment is also calculated as support span length (L) multiplied by the applied load (N), except that these values are obtained from the yield point, rather than the ultimate point.

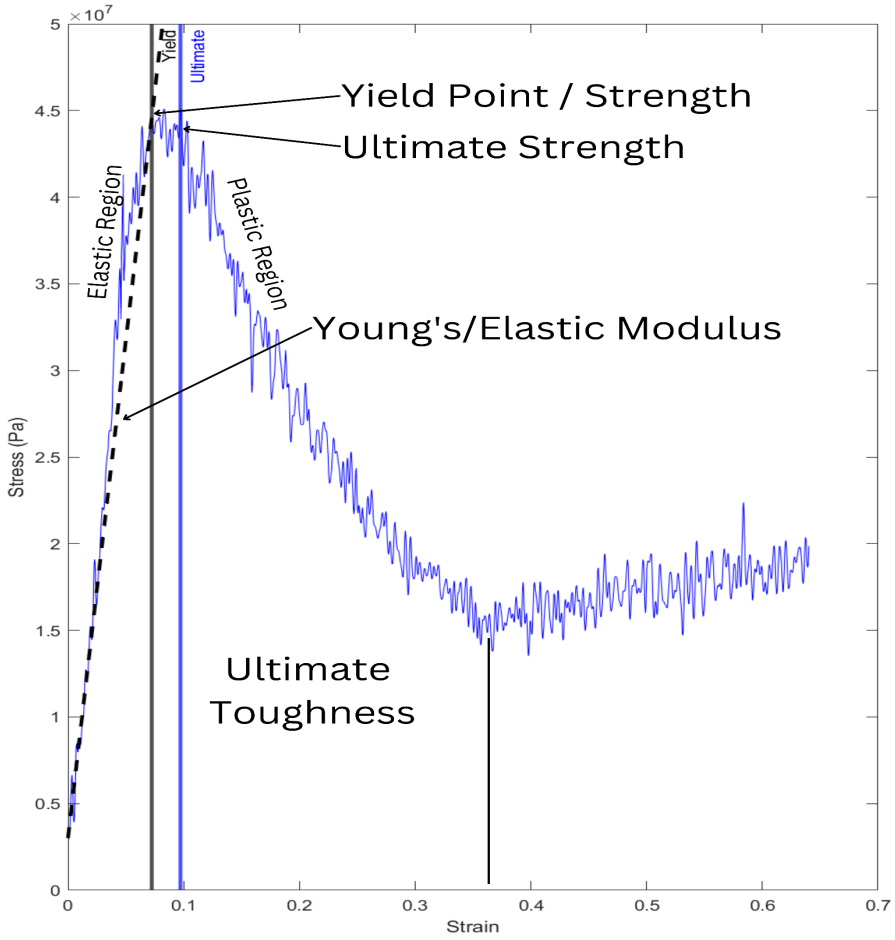

Figure 1: Specimen 3018 - Femur stress vs strain graph.

Statistical Tests:

For each individual specimen, geometric and material property values for the right and left bones were averaged together. The bones used include the humerus, femur, radius, and tibia. Direct comparisons were made between the humerus and femur and between the radius and tibia within each sample, given that these bones are developmentally homologous. Since the ages of the samples differed, each specimen's hindlimb bone was only compared to its own forelimb bone. Therefore, paired statistical tests were used. Binomial and Wilcoxon's tests are used to determine if any statistically significant differences between the robustness of the hind and forelimb exist within each sample. The statistical software used was R (v4.1.2; R Core Team 2021). The R code was written by JWY and generated the p-values from the right-tailed binomial and Wilcoxon tests. The p-value from the R output is shown in **Table 2**. Additionally, R generated graphs for each of the binomial tests. Each graph shows a line with a slope of one with the forelimb on the x-axis and the hindlimb on the y-axis. Those specimens shown above the line have more robust hindlimbs than forelimbs and those specimens shown below have more robust forelimbs than hindlimbs. Examples of these graphs are shown in **Figures 2, 3, and 4.**

Results:

As shown in **Table 2** and **Table 3**, significant differences could only be found for geometric properties, but none were found for any material or whole bone properties. Results differed between the proximal and distal limbs.

For the distal limb comparison, a significant difference could be observed in both geometric properties. Both the cross-sectional area and polar selection modulus were significantly greater in the tibia when compared to the radius. The tibia was found to be more robust in all 8 samples tested. This produced a p-value of p=0.0039 for both Z_{pol} and CSA.

These results are shown in **Figures 2 and 3**. No significant differences were found for the material properties such as elastic modulus (p=0.7187), bone mineral density (p=0.1914), ultimate strength (p=1), yield strength (p=1), or ultimate toughness (p=1). While significant differences in material properties could not be found, predicted patterns were nonetheless discernible. For example,of the eight individuals for which we could obtain values for both tibial and radial BMD, six displayed greater BMD in the tibia. Significant values were not observed in either of the whole bone properties examined. Both the ultimate moment (p=0.1563) and yield moment (p=0.6562) were not significantly different between the tibia and radius. However, the ultimate moment (p= 0.1563) also showed a trend with 4 of 6 samples displaying greater values in the tibia.

Property	Wilcox Test	Binomial Test
Cross-Sectional Area	0.0039	0.0039
Z_{pol}	0.0039	0.0039
Elastic Modulus	0.7187	0.8906
Bone Mineral Density	0.1914	0.1445
Ultimate Strength	1	1
Yield Strength	1	1
Ultimate Toughness	1	1
Ultimate Moment	0.1563	0.3438
Yield Moment	0.6562	0.6563

Table 2: P-value for the radius vs tibia. The significant values are shown in red (α=0.05).

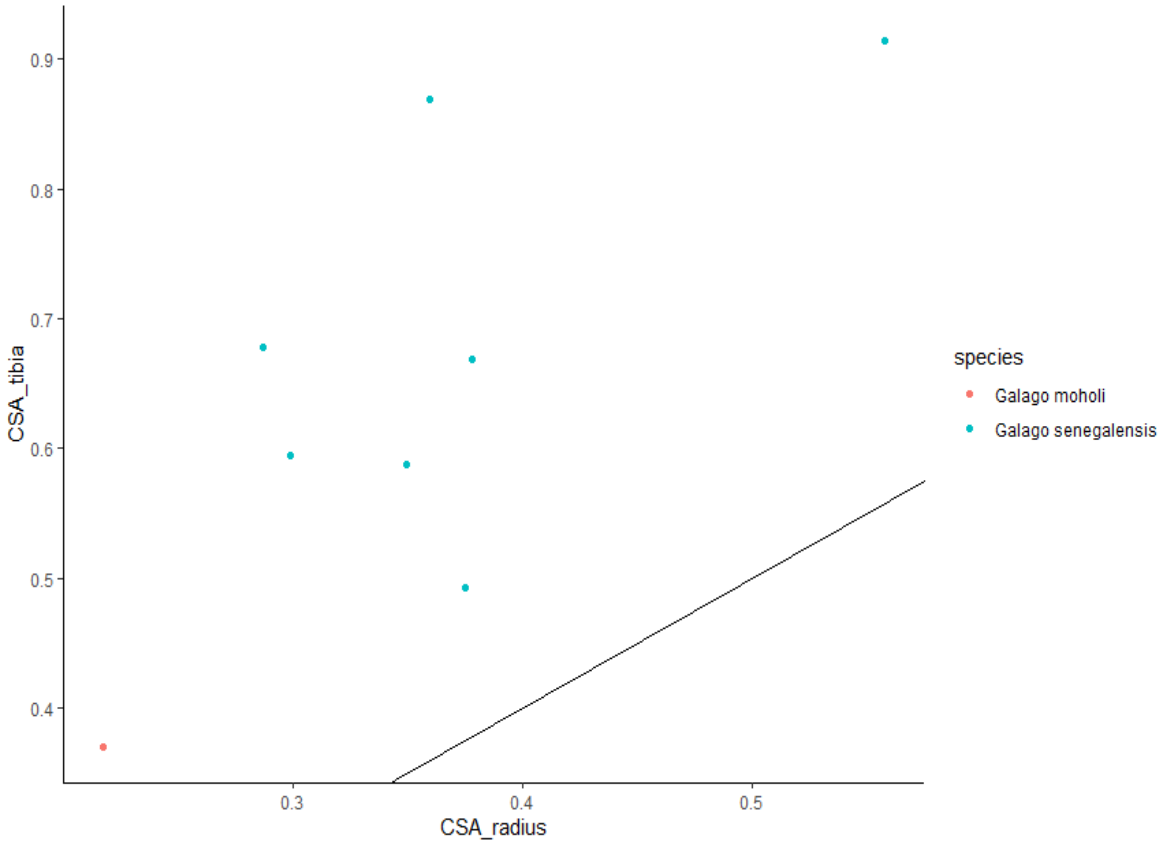

Figure 2: Graphical output from R for CSA comparison for radius vs tibia. The slope of line = 1. Values above the line indicate that the hindlimb is more robust than the forelimb. p= 0.0039. Orange dots indicate the species *Galago mohonli* and blue does indicate *Galago senegalensis*.

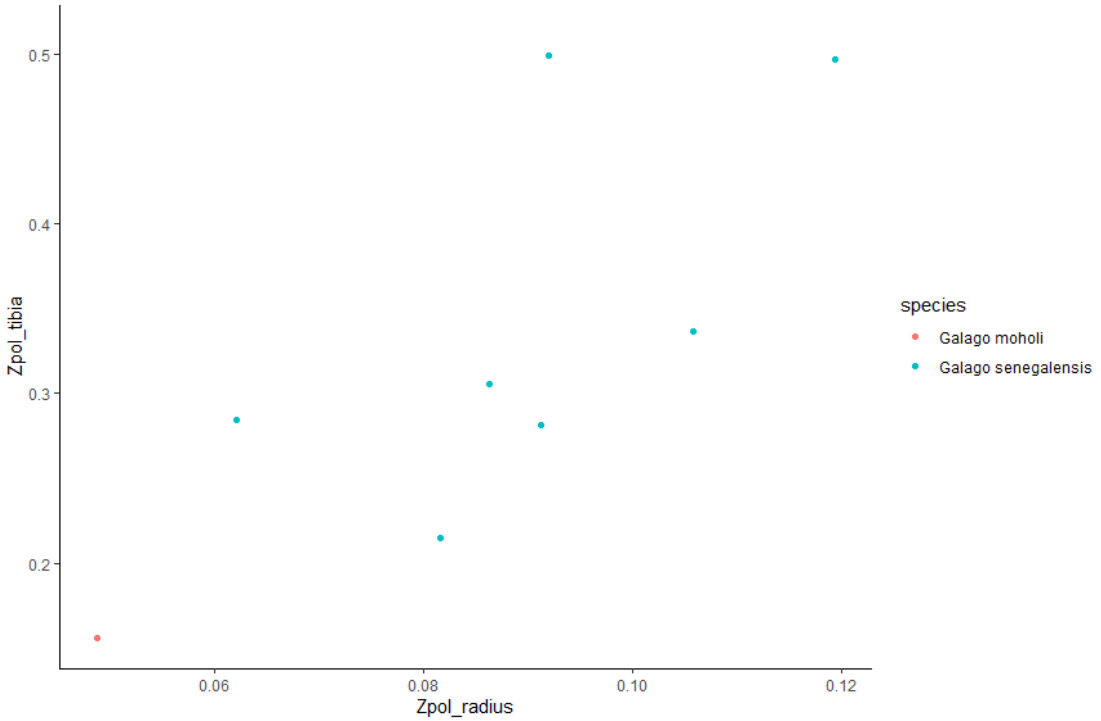

Figure 3: Graphical output from R for Z_{pol} comparison for radius vs tibia. Slope of 1 is not displayed on graph, due to the scale of the x- and y-axes. p-value= 0.0039. Orange dots indicate the species *Galago moholi* and blue does indicate *Galago senegalensis*.

For the proximal bone comparison, a significant difference could be observed only in the polar section modulus (Z_{pol}). This result is shown in **Figure 4.** Unlike the distal bone comparison, CSA was not significantly different with a p-value of 0.1484. No significant differences were found for the material properties such as elastic modulus (p=0.0625), bone mineral density (p=0.1484), ultimate strength (p=0.6875), yield strength (p=0.6875), or ultimate toughness (p=1). While significant differences in material properties could not be found, some had values near significance. For example, the elastic modulus displayed a value of p=0.0625. Of the four samples, all four displayed greater elastic modulus in the femur, suggesting limited statistical power. Significant values could not be observed in either whole bone properties. Both the

ultimate moment (p=0.1563) and yield moment (p=0.6562) were not significantly different between the humerus and femur. However, the ultimate moment (p=0.1250) was near significance with the 4/6 sample displaying greater values in the femur.

Property	Wilcox Test	Binomial Test
Cross-Sectional Area	0.1484	0.5000
Zpol	0.0078	0.0078
Elastic Modulus	0.0625	0.0625
Bone Mineral Density	0.1484	0.2266
Ultimate Strength	0.6875	0.6875
Yield Strength	0.6875	0.9375
Ultimate Toughness	1	1
Ultimate Moment	0.1250	0.3125
Yield Moment	0.4375	0.6875

Table 3: P-value for the humerus vs femur. The significant values are shown in red (α=0.05).

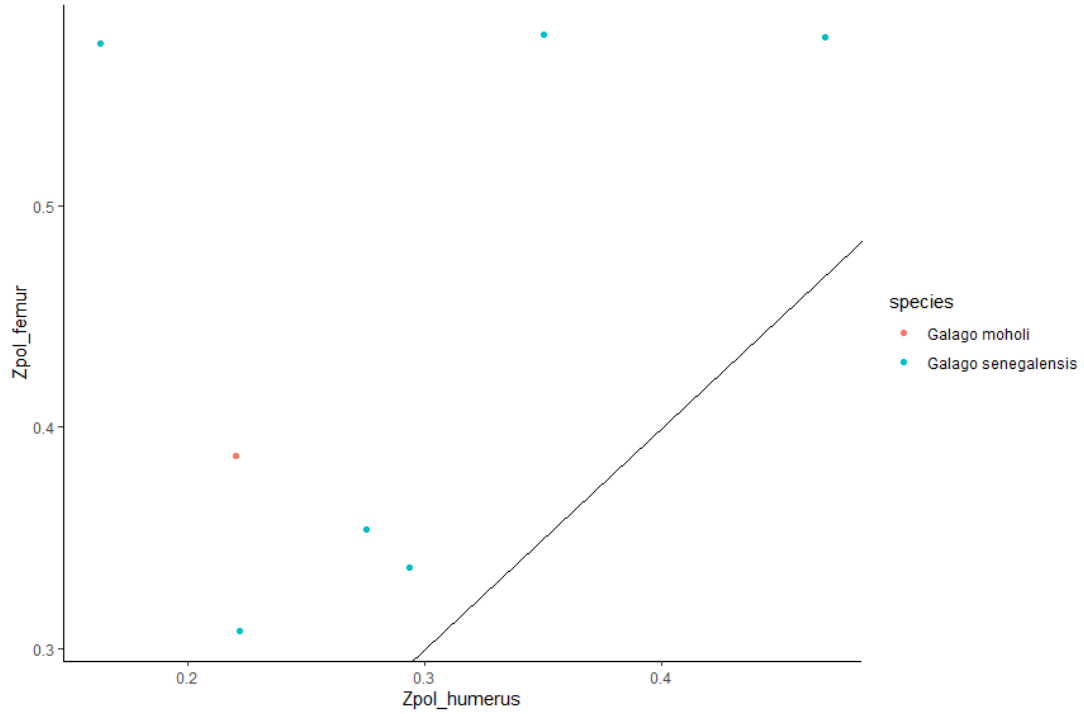

Figure 4: Graphical output from R for Z_{pol} comparison of humerus vs femur. A slope of 1 is not displayed on the graph. p-value= 0.0078. Red dots indicate the species *Galago moholi* and blue does indicate *Galago senegalensis*.

Discussion:

Significant differences were observed for geometric properties such as Z_{pol} and CSA in the distal limbs. However, in the proximal limb comparison, only the Z_{pol} was found to be significant. This study did not find any significant differences in either whole bone properties or material properties in either the distal or proximal limb comparisons.

The results of this study closely align with previous findings from Young et al. (2018). *Propithecus coquereli*, a leaping primate, was found to have a more robust femur than humerus in geometric properties. This aligns with the findings of this study as the Z_{pol} was found to be greater for the femur than for the humerus. However, the Young et al. study also found that *P.*

coquereli displayed a greater CSA in the femur compared to the humerus. This finding could not be replicated in this study of *G. moholi* and *G. senegalensis*. No significant difference was observed in CSA for the proximal bone comparisons. The Young et al. (2018) study did not observe any differences in whole bone properties or material properties between leaping and quadrupedal primates. This aligns with the results of this study, which also found that the method of locomotion did not have a relationship with material or whole bone properties. Additionally, these findings align with Terranova, which found that leaping primates display more robust femoral and tibial mid-shift when compared to non-leaping primates (1995). This study finds similar results, with the tibia and femur displaying more robust geometric properties. Both studies conclude a relationship between locomotion and the geometric properties of bone.

Limitations:

One important limitation of this study was the sample size. Only 12 specimens were available and not all bones present could be extracted without damage. A total of 12 specimens were obtained and each specimen could potentially have yielded 4 bones for testing: tibia, radius, humerus, and femur. However, difficulty in extraction meant that many bones were too damaged to be scanned or subjected to the three-point bend test. Additionally, some bones were removed from the sample due to size. Bones too short to be supported by the three-point bend flexure fixtures were excluded from the sample.

This low sample number created difficulty in finding significant differences even when properties were different in all specimens. Some properties, such as the elastic modulus in the proximal limbs ($p=0.065$), displayed a greater value for the hindlimbs in all samples but could not be considered significant due to the small number of usable samples. BMD displayed a

greater value for 5/7 of samples in both the proximal and distal limbs. Low statistical power meant that many of these material properties may have differed but this cannot be concluded from this data due to a low number of samples.

Conclusions:

This study contributed to existing research showing that differences in geometric properties are present in primates before they could be subject to significant loading stress. This indicates that these geometric differences result from genetic or epigenetic factors rather than bone functional adaptation. This research strengthens our understanding of the factors that shape bone morphology and demonstrates that both genetics and loading history environment play a role in bone cortical robustness.

References

Aerts, P. (1998). Vertical jumping in galago senegalensis: The quest for an obligate mechanical power amplifier. *Philosophical Transactions of the Royal Society of London. Series B: Biological Sciences*, *353*(1375), 1607–1620. https://doi.org/10.1098/rstb.1998.0313

Biewener AA, Taylor CR. 1986. Bone strain: a determinant of gait and speed? J Exp Biol 123:383–400

Connour JR, Glander K, Vincent F. 2000. Postcranial adaptations for leaping in primates. J Zool 251:79–103

Doube M, Klosowski MM, Arganda-Carreras I, Cordelières F, Dougherty RP, Jackson J, Schmid B, Hutchinson JR, Shefelbine SJ. 2010. BoneJ: free and extensible bone image analysis in ImageJ. Bone 47:1076–1079

Hall-Craggs, E. B. C. 1965 An analysis of the jump of the lesser galago (Galago senegalensis). 7. Zool. 147, 2

Masters, J.C.; Génin, F.; Couette, S.; Groves, C.P.; Nash, S.D.; Delpero, M.; Pozzi, L. (2017). "A new genus for the eastern dwarf galagos (Primates: Galagidae)". Zoological Journal of the Linnean Society. 181 (1): 229–241.

Florencio-Silva, R., Sasso, G. R., Sasso-Cerri, E., Simões, M. J., & Cerri, P. S. (2015). Biology of bone tissue: Structure, function, and factors that influence bone cells. *BioMed Research International*, *2015*, 1–17. https://doi.org/10.1155/2015/421746

Robling, A. G., Hinant, F. M., Burr, D. B., & Turner, C. H. (2002). Improved bone structure and strength after long-term mechanical loading is greatest if loading is separated into short bouts. *Journal of Bone and Mineral Research*, *17*(8), 1545–1554. https://doi.org/10.1359/jbmr.2002.17.8.1545

Ruff, C., Holt, B., & Trinkaus, E. (2006). Who's afraid of the big bad wolff?: “Wolff's law” and Bone functional adaptation. *American Journal of Physical Anthropology*, *129*(4), 484–498. https://doi.org/10.1002/ajpa.20371

Saunders, M. M., & Donahue, H. J. (2004). Development of a cost-effective loading machine for biomechanical evaluation of Mouse Transgenic models. *Medical Engineering & Physics*, *26*(7), 595–603. https://doi.org/10.1016/j.medengphy.2004.04.005

Warden, S. J., Hurst, J. A., Sanders, M. S., Turner, C. H., Burr, D. B., & Li, J. (2004). Bone adaptation to a mechanical loading program significantly increases skeletal fatigue resistance. *Journal of Bone and Mineral Research*, *20*(5), 809–816. https://doi.org/10.1359/jbmr.041222

Rasband WS. 1997–2007. ImageJ. Bethesda, MD: U.S. National Institutes of Health http://rsb.info.nih.gov/ij/.

Terranova CJ. 1995. Leaping behaviors and the functional morphology of strepsirrhine primate long bones. Folia Primatol (Basel) 65:181–201

Turner CH, Burr DB. 1993. Basic biomechanical measurements of bone: a tutorial. Bone 14:595–608

Young, J. W., Jankord, K., Saunders, M. M., & Smith, T. D. (2018). Getting into shape: Limb bone strength in perinatal lemur *catta* and *propithecus coquereli*. *The Anatomical Record*, *303*(2), 250–264. https://doi.org/10.1002/ar.24045

Comparison of Bone Robustness Between Fore- and Hindlimb

in Neonatal and Infant *Galago*

Jeremy Busken

Department of Biology

Honors Research Project

Submitted to

The Williams Honors College
The University of Akron

Approved:

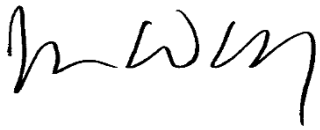

Honors Project Sponsor (signed)

Dr. Jesse Young 4/25/2023

Honors Project Sponsor (printed) Date

Honors Project Reader (signed)

Dr. Brian Bagatto 4/27/2023

Honors Project Reader (printed) Date

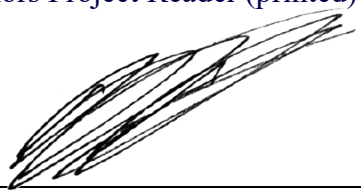

Honors Project Reader (signed)

Dr. Henry Astley 4/26/23

Honors Project Reader (printed) Date

Accepted:

Honors Faculty Advisor (signed)

Dr. Brian Bagatto 4/27/2023

Honors Faculty Advisor (printed) Date

Department Chair (signed)

Dr. Stephen Weeks 4/28/2023

Department Chair (printed) Date